

# Effect of Spray Drying Conditions on Physical Properties of *Panax notoginseng* Saponin (PNS) Powder and the Intra-Batch Dissolution Variability of PNS Hydrophilic Matrix Tablet

This article was published in the following Dove Press journal:  
*Drug Design, Development and Therapy*

Maorui Yang<sup>1</sup>  
Bing Xu<sup>1,2</sup>  
Xin Wang<sup>1</sup>  
Wanting Li<sup>1</sup>  
Junjie Cao<sup>1</sup>  
Wenjing Li<sup>1</sup>  
Yanjiang Qiao<sup>1,2</sup>

<sup>1</sup>Department of Chinese Medicine Informatics, Beijing University of Chinese Medicine, Beijing, People's Republic of China; <sup>2</sup>Beijing Key Laboratory of Chinese Medicine Manufacturing Process Control and Quality Evaluation, Beijing, People's Republic of China

**Purpose:** Understanding raw material variability and its impact on product quality are crucial for developing robust pharmaceutical processes. This work aimed to study the effects of spray drying conditions on properties of the spray dried *Panax notoginseng* saponin (PNS) powders as well as the subsequent intra-batch dissolution variability of PNS hydrophilic matrix tablets.

**Methods:** The Plackett-Burman design was applied to screen the critical process parameters (CPPs). Then, the Box-Behnken design was used to investigate the relationship between the CPPs and the physicochemical properties of spray dried PNS powders. The PNS hydrophilic matrix tablets containing 57% spray dried PNS powders were directly compressed. The partial least squares (PLS) regression was used to uncover the hidden multivariate relationships among the CPPs, intermediate powder properties, and tablet quality attributes.

**Results:** The identified CPPs were the feed concentration, the inlet air temperature, and the atomization pressure. It was found that the CPPs exerted little impact on chemical properties of spray dried PNS powders, but had significant impact on physical properties, such as particle size, specific surface area, bulk density, hygroscopicity, and inter-particle porosity, etc. Latent variable modeling results revealed that the high inlet air temperature of spray drying process could produce PNS powders with low moisture content and high hygroscopicity, which were beneficial to reduce the intra-batch dissolution variability of PNS hydrophilic matrix tablets. Finally, a design space of the spray drying process was built in order to ensure the dissolution consistency.

**Conclusion:** Our research provided a reference for improving the spray drying conditions in order to ensure the dissolution consistency of the PNS hydrophilic matrix tablet.

**Keywords:** spray drying, *Panax notoginseng* saponin, hydrophilic matrix tablet, dissolution variability, quality by design

## Introduction

According to the World Health Organization (WHO), cardiovascular disease (CVD) is the number one cause of death globally. In 2016, an estimated 17.9 million people died from CVDs, accounting for 31% of all global deaths.<sup>1</sup> Drug intervention therapy has low cost and plays an important role in prevention and treatment of CVDs. The drugs currently used for CVDs include aspirin, statins, and clopidogrel. However, long-term use or large amounts of aspirin could cause gastrointestinal

Correspondence: Bing Xu; Yanjiang Qiao  
Department of Chinese Medicine Informatics, Beijing University of Chinese Medicine, No. 11, North Third Ring East Road, Beijing City, 100029, People's Republic of China  
Email xubing@bucm.edu.cn; yjqiao@bucm.edu.cn

reactions, and in severe cases, upper gastrointestinal bleeding.<sup>2</sup> Clopidogrel is widely used in thrombotic diseases, but acute or long-term use may also cause bleeding.<sup>3</sup> Statins are associated with adverse reactions, ie, muscle pain.<sup>4</sup> For patients with CVDs, long-term medication is usually implemented, so the probability of adverse drug reactions increases. At present, there is growing interest in using traditional Chinese medicine to treat CVDs. *Panax notoginseng* is the dried root and rhizome of the Araliaceae plant *Panax notoginseng* (Burk.) F. H. Chen.<sup>5</sup> *Panax notoginseng* saponins (PNS) are extracted from *Panax notoginseng*, which can protect the myocardium, resist arrhythmia, and reduce arterial blood pressure.<sup>6</sup> The major active pharmaceutical ingredients (APIs) of PNS include ginsenoside Rg<sub>1</sub>, ginsenoside Rb<sub>1</sub>, ginsenoside Re, ginsenoside Rd, notoginsenoside R<sub>1</sub>, etc. Ginsenoside Rb<sub>1</sub> and Rg<sub>1</sub> can activate NO by regulating the PI3K/Akt/eNOS pathway, increase endothelium-dependent vasodilation, and prevent thrombosis.<sup>7</sup> Notoginsenoside R<sub>1</sub> can improve the morphological changes of damaged mitochondria, reduce oxidative stress and inflammation, and prevent myocardial ischemia or reperfusion injury through the VDUP1 pathway and NF- $\kappa$ B pathway.<sup>8</sup> Besides, a combination usage of PNS and chemical medicines in treatment of CVDs was reported to reduce gastrointestinal damage compared to single usage of aspirin.<sup>9</sup>

At present, PNS are mainly used as the drug materials of Xuesaitong or Xueshuantong injections and immediate release (IR) tablets on the market.<sup>10,11</sup> The injections can increase bioavailability and enhance efficacy, but there is a risk of adverse drug reactions.<sup>12</sup> The IR tablet form is preferred since it is easy to take and disintegrates quickly, but it has the disadvantages of incomplete absorption and low bioavailability.<sup>13</sup> The controlled release dosage forms can effectively deliver the drug, improve bioavailability, reduce the frequency of drug application, and improve safety. In a case, a new type of PNS colon-specific osmotic pump controlled-release capsule was reported to enhance the permeability of the drug in a Beagle dog. Compared with ordinary PNS capsules, the relative bioavailability of this new capsule reached 487.42%.<sup>14</sup> The hydrophilic matrix tablet prepared with HPMC is the ideal choice for oral extended release dosage form,<sup>15–17</sup> which has advantages in regulatory status, simple technology, cost savings, and relative inertness of polymers.<sup>18,19</sup> For example, the PNS bio-adhesive pellets that had HPMC applied as the adhesive material had the highest bioavailability in rats

compared to other adhesive materials.<sup>20</sup> Peng first carried out in vitro and in vivo pharmacokinetic evaluation of PNS hydrophilic matrix tablets in domesticated rabbits, and the results confirmed that PNS sustained release tablets showed obvious release effect.<sup>21</sup>

Understanding raw material variability and its impact on processability and product quality are crucial for developing robust pharmaceutical formulations and processes. Stauffer et al<sup>22</sup> revealed that the crystal length, agglomerate size, and flowability parameters were main sources of inter-batch variability of APIs. These factors further affected continuous manufacturing processes such as feeding, mixing, granulation, and compression. For example, if the agglomerates were not well-dispersed during the mixing step, the content uniformity of tablets would be at risk. Thoorens et al<sup>23</sup> studied the effect of batch-to-batch variability of microcrystalline cellulose (MCC) on tabletability. The results of principal component analysis (PCA) showed that MCC materials from different sources had obvious clustering trends, and the moisture content between clusters was different, which led to different tensile strengths of tablets. Our previous studies also showed that the batch-to-batch or vender-to-vender variability of APIs and excipients could influence the dissolution profiles of PNS hydrophilic matrix tablets.<sup>24,25</sup>

The properties of powdered raw materials are largely affected by processing conditions during their preparation. Spray drying is often used as a method for powder preparation because of its simple operation, short drying time, and good drying effect.<sup>26</sup> As required by the principles of quality by design (QbD), it is important to study the effects of changes in critical process parameters (CPPs) and critical material attributes (CMAs) on the critical quality attributes (CQAs) of the final product.<sup>27</sup> A lot of research showed that spray drying process parameters such as the atomization pressure, the inlet air temperature, the air flow, and the feed rate had great influences on physical and chemical properties of spray dried powders.<sup>28,29</sup> For instance, Asun et al found that increasing the inlet air temperature resulted in coconut sugar powders with high flowability and wettability.<sup>30</sup> Tontul et al proved that atomization pressure was the most effective parameter influencing particle size and other physical properties of the powder.<sup>31</sup> Besides, Rattes et al<sup>32</sup> studied the influence of spray drying conditions during the formation of sodium diclofenac microparticles. It was found that the feed flow rate had the greatest impact on in vitro dissolution, and

a higher feed flow rate could result in a slower release rate of microencapsulating composition.

The aim of this work was to illustrate the relationship between the CPPs of spray drying process and the quality attributes of spray dried PNS powder. The prepared PNS powders were then directly compressed into hydrophilic matrix tablets, and the impact of spray drying CPPs on intra-batch dissolution variability was also investigated. As far as we know, there are currently few articles studying the influence of spray drying process parameters on the intra-batch drug release uniformity. Finally, a spray drying design space was suggested in order to obtain robust drug dissolution.

## Materials and Methods

### Materials

The names, lot numbers, and suppliers of materials used in the experiment are shown in Table 1. No. 1–6 materials represent the *Panax notoginseng* saponins and reference substances of five APIs. No. 7–10 materials correspond to the excipients in the tablet formulation.

### Preparation and Characterization of Spray Dried PNS Powders

#### Experimental Design

According to literature reports,<sup>28,33–35</sup> the feed concentration, feed flow rate, atomization pressure, inlet air temperature, and air flow rate that affected the spray-dried powder properties were determined as potential critical process parameters (pCPPs). In order to screen out critical process parameters by the least number of experiments, the Plackett-Burman design was used on Design Expert software (Stat-Ease Inc., Minneapolis, Minnesota, USA). Factors and levels of the Plackett-Burman design are listed in Table 2. The spray drying process was operated at different feed concentrations (0.2 and 0.4 g/mL), inlet air temperatures (160 and 240°C), feed flow rates (300 and 500 mL/h), air flow rates (40 and 60 m<sup>3</sup>/min), and atomization pressures (0.1 and 0.3 MPa). These conditions were used as independent variables and the physical and chemical properties of the spray dried powders were used as response variables. The effects of independent variables on each response variable were modeled by the multiple linear regression (MLR) equation as described in Equation (1).

$$Y = \beta_0 + \beta_1 X_1 + \beta_2 X_2 + \beta_3 X_3 + \beta_4 X_4 + \beta_5 X_5 \quad (1)$$

The Box-Behnken design is a multi-factor, three-level experimental design method, and it is commonly used in

**Table 1** The Information of Materials

No.	Name	Lot Number	Supplier
1	<i>Panax notoginseng</i> saponin	20170910	Nanjing Zelang Biotechnology Co., Ltd. (Jiangsu, P.R. China)
2	Notoginsenoside R <sub>1</sub>	4196	Shidande Biotechnology Co., Ltd (Shanghai, P.R. China).
3	Ginsenoside Rg <sub>1</sub>	4628	Shidande Biotechnology Co., Ltd (Shanghai, P.R. China).
4	Ginsenoside Rd	4899	Shidande Biotechnology Co., Ltd (Shanghai, P.R. China).
5	Ginsenoside Re	5121	Shidande Biotechnology Co., Ltd (Shanghai, P.R. China).
6	Ginsenoside Rb <sub>1</sub>	4976	Shidande Biotechnology Co., Ltd (Shanghai, P.R. China).
7	HPMC K4M	3D13012N010	Dow Chemical Company (Michigan, USA)
8	HPMC K15M	ID10012N02	Dow Chemical Company (Michigan, USA)
9	Lactose	F20120009	DFE Pharmaceutical Company (Kapuni, Netherlands)
10	Magnesium stearate	20121010	Sino Pharm Chemical Reagent Co., Ltd (Shanghai, P.R. China).

response surface methodology. Based on the results of the Plackett-Burman design, the Box-Behnken design was used to optimize the critical process parameters. Table 3 shows the factors and levels of the Box-Behnken design.

### Spray Drying Conditions

Prior to the experiments, about 200 g of PNS powders were dispersed and dissolved in deionized water under magnetic stirring for 10 min. Different amounts of deionized water were used to prepare feed solutions with concentrations of 0.2, 0.3, and 0.4 g/mL,

**Table 2** Factors and Levels for the Plackett-Burman Design

Variable	Process Parameter	Unit	Levels	
			Low (-1)	High (+1)
X <sub>1</sub>	Feed concentration	g/mL	0.2	0.4
X <sub>2</sub>	Feed flow rate	mL/h	300	500
X <sub>3</sub>	Atomization pressure	MPa	0.1	0.3
X <sub>4</sub>	Inlet air temperature	°C	160	240
X <sub>5</sub>	Air flow rate	m <sup>3</sup> /min	40	60

**Table 3** Factors and Levels for the Box-Behnken Design

Variable	Process Parameter	Unit	Levels		
			Low (-1)	Mid (0)	High (+1)
X <sub>1</sub>	Feed concentration	g/mL	0.2	0.3	0.4
X <sub>3</sub>	Atomization pressure	MPa	0.1	0.2	0.3
X <sub>4</sub>	Inlet air temperature	°C	160	200	240

respectively, according to the experimental design. The spray drying process was carried out using a YC-015 lab spray dryer (Pilotech Instrument Equipment, Shanghai, P.R. China). The spray dryer was operated concurrently with a two-fluid nozzle with an orifice of 1.0 mm in diameter.

### High Performance Liquid Chromatography Analysis

The assay of APIs was performed on a high performance liquid chromatography (HPLC) system (Agilent, USA) which was equipped with a quaternary pump (G1311B), a column oven (G1316A), and a VL diode array detector (G1315D). The chromatographic separation was carried out on a reversed phase column (250 mm×4.6 mm, ZORBAX SB-C18) with the mobile phase consisting of acetonitrile and water and the following gradients: 0 min, 20:80 (v/v); 20 min, 20:80 (v/v); 50 min, 47:53 (v/v). The flow rate was maintained at 1.0 mL/min. The detection wavelength was 203 nm and the column temperature was 23°C. All sample solutions were filtered through a membrane filter (0.45 μm) before injection into the HPLC system.

### Characterization of Physical Properties of Spray Dried PNS Powder

The major indices used to assess the spray dried powders included moisture content, hygroscopicity, specific surface area, particle size and distribution, density and porosity parameters, flowability parameters, and glass transition temperature.

#### Moisture Content

The moisture content (MC) of spray dried PNS powder was determined on a rapid moisture analyzer (MA 35, Sartorius Scientific Instrument, Göttingen, Germany). Approximately 2.0 g of the spray dried PNS powder was placed in the aluminum testing pan and dried at 105°C for 10 min. Each sample was tested in triplicate, and the average value of three measurements was used.

#### Hygroscopicity

The dry weighing bottle was placed in a desiccator (sodium chloride saturated solution was placed at the bottom) at constant temperature of 22±2°C for 12 h. The spray dried PNS powders were placed into the bottle, and the thickness of powder was about 1 mm. The hygroscopicity (H) was the percentage increase in sample weight at a certain temperature and humidity after 24 h.

#### Specific Surface Area

The specific surface area (SSA) of spray dried PNS powder was determined using a specific surface and aperture analyzer (3H-2000PS1, Bei Shi de Instrument Technology Co., Ltd, Beijing, P.R. China). The analysis was based on the Brunauer-Emmett-Teller (BET) adsorption isotherm.

#### Particle Size Distribution Width

The particle size distribution of spray dried PNS powder was analyzed by a laser diffraction particle size analyzer (BT-2001, Dandong Baite Instrument Co., Ltd., Dandong, P.R. China). The  $D_{10}$ ,  $D_{50}$ , and  $D_{90}$  respectively refers to the particle size value of 10%, 50%, and 90% percentage of cumulative distribution. The particle size distribution width (*Span*) value was calculated as shown in Equation (2). Each sample was tested in triplicate.

$$Span = \frac{D_{90} - D_{10}}{D_{50}} \quad (2)$$

#### Bulk and Tapped Densities

About 100.0 g (*m*) samples were poured slowly into the cylinder (250 mL) through the funnel. The surface of the powder bed was slightly smoothed, and the volume (*V<sub>a</sub>*)

was recorded. Then, the cylinder was fixed on a powder density tester (HY-100, Dandong Hao Yu Technology Co., Ltd., Dandong, P.R. China), and the volume ( $V_c$ ) was read after 1250 times of vibrations. Each sample was tested in triplicate.

The bulk density ( $D_a$ ) was calculated using Equation (3).

$$D_a = \frac{m}{V_a} \quad (3)$$

The tapped density ( $D_c$ ) was calculated using Equation (4).

$$D_c = \frac{m}{V_c} \quad (4)$$

### Inter-Particle Porosity (Ie), Carr Index (IC), and Hausner Index (IH)

These parameters were calculated based on the bulk density and the tapped density according to the following equations.

$$I_e = \frac{D_c - D_a}{D_c \times D_a} \quad (5)$$

$$IC = \frac{D_c - D_a}{D_c} \times 100 \quad (6)$$

$$IH = \frac{D_c}{D_a} \quad (7)$$

### Cohesion Index

The cohesion index ( $I_{cd}$ ) was determined by measuring the average hardness of tablets obtained by compression of powders under eccentric pressure. The powder was compressed into tablets on an automatic tablet press (ZYP-30TS, Xinnuo Instrument Group Co., Ltd., Shanghai, P.R. China), and the tablet size was 10 mm in diameter. Each sample was tested in triplicate.

### Angle of Repose

About 100 g of spray dried PNS powders was slowly added from the funnel, and gradually accumulated on the bottom disc until a stable cone was formed. The height of the cone ( $h$ ) and the radius of the bottom disc ( $r$ ) were recorded. The angle of repose ( $\alpha$ ) was calculated using the following equation. Each sample was tested in triplicate.

$$\alpha = \arctan \frac{h}{r} \quad (8)$$

### Skeleton Density

The skeleton density ( $D_s$ ) was determined by an automatic specific surface area and pore size analyzer (3H-2000A,

Beishide Instrument Technology Co., Ltd., Beijing, P.R. China). First, the empty tube volume of the sample (with the filling rod) was measured and recorded as  $V_1$ . The sample weight ( $m$ ) was accurately weighed by weight loss method, and the volume ( $V_2$ ) of tube containing the sample was measured by helium gas. The skeleton density was calculated using Equation (9). In order to eliminate the influence of moisture, the spray dried PNS powders were placed in a desiccator for 24 hours, before the skeletal density was measured.

$$D_s = \frac{m}{V_1 - V_2} \quad (9)$$

### Glass Transition Temperature

The glass transition temperature ( $T_g$ ) of spray dried PNS powder was measured by a differential scanning calorimeter (TA Instruments Q2000, New Castle, USA), which was equipped with TA universal analysis software. About 5–7 mg of the spray dried PNS powders was added to the T-zero aluminum pan. Subsequently, it was heated from 10°C to 220°C at the rate of 10°C/min, and the nitrogen purge rate was 50 mL/min.

### Preparation of PNS Hydrophilic Matrix Tablets

The formulation of PNS hydrophilic matrix tablets was composed of 57% (w/w) spray dried PNS, 23% (w/w) lactose, 19% (w/w) HPMC K4M, and 1% (w/w) HPMC K15M. The mixture was uniformly blended by an equal increment method. Then, 0.3% (w/w) magnesium stearate was added, and the mixture was uniformly blended again. The punch diameter of the rotary tablet press (ZP10, Xinyuan Pharmaceutical Machinery Co., Ltd., Shanghai, P.R. China) was 10 mm. The PNS powder was filled into the die manually, and six PNS hydrophilic matrix tablets were prepared for every batch.

### In vitro Dissolution Test

According to the United States Pharmacopeia (USP),<sup>36</sup> the dissolution profile of tablets was tested by the basket method using a dissolution tester (RC-806D, Tiandatianfa Technology Co., Ltd., Tianjin, P.R. China). The rotation speed was set at 100 r/min, and 500 mL deionized water was used as the medium at 37±0.5°C.<sup>24</sup> The dissolution medium with dissolved APIs was sampled at 1 h, 2 h, 4 h, 6 h, 8 h, and 12 h, respectively. The sample solution was filtered by using a microporous membrane (0.45 μm) and

was then analyzed by HPLC. The cumulative release of each API was calculated at each time point as follows:

$$X_n = C_n V_n + 1 \cdot \sum_n^{n-1} C_i * V_i \quad (10)$$

$$F = \frac{X_n}{M} \times 100\% \quad (11)$$

Where  $C_n$  is the drug concentration,  $V_n$  is the drug volume,  $F$  is the cumulative release of the drug,  $X_n$  is the release amount, and  $M$  is the drug content.

## Results and Discussion

### Identification of Critical Process Parameters

According to the Plackett-Burman design in Preparation and Characterization of Spray Dried PNS Powders, 12 batches of PNS powders prepared under different conditions were obtained. The contents of five APIs in PNS powder were determined by HPLC according to Preparation and Characterization of Spray Dried PNS Powders. Table 4 shows the contents of five APIs as well as the content of total saponins. The content ranges were 8.35–9.33%, 28.31–32.68%, 2.64–4.58%, 32.23–36.06%, 7.92–8.67%, and 80.39–91.52% for notoginsenoside  $R_1$ , ginsenoside  $R_{g1}$ , ginsenoside  $R_e$ , ginsenoside  $R_{b1}$ , ginsenoside  $R_d$  and total saponins, respectively. For each API, the ratio of the maximum content value to the minimum (Max/Min) was close to 1, indicating that the contents did not change much among 12 batches. Furthermore, the MLR models were built for each API as well as the total saponins, and analysis of variance (ANOVA) was carried

out. The results showed that p-values of all models were greater than 0.05, demonstrating that different process parameters did not affect chemical quality attributes of the spray dried PNS powders.

According to our previous research,<sup>24</sup> the physical quality attributes of powders affecting the dissolution of PNS matrix tablet were the moisture content (MC), hygroscopicity (H), specific surface area (SSA), and particle size distribution width (Span). Therefore, the four physical quality attributes were characterized as shown in Table 5. Besides, the yield was given to evaluate the efficiency of the spray drying process. For four physical quality attributes, the Max/Min values ranged from 1.42 to 5.50, which were all larger than that of chemical quality attributes. The MLR and ANOVA were performed on each physical quality attribute as well as the yield. It was suggested that a good regression model should have  $R^2$  no less than 80%,<sup>37</sup> and the p-value of model should be less than 0.05. The fitting results illustrated that the yield, hygroscopicity, and particle size distribution width could not be fitted well (i.e.,  $R^2 = 0.4274$ ,  $0.5494$ , and  $0.4532$ , respectively, and p-values of model were 0.5383, 0.3255, and 0.4919, respectively). On the contrary, good MLR models were obtained for MC ( $R^2 = 0.8359$ , and p-value of model equals 0.0238) and SSA ( $R^2 = 0.9275$ , and p-value of model equals 0.0023), as shown below.

$$MC = 8.151 + 1.681X_1 + 0.003X_2 - 0.069X_3 - 0.017X_4 - 0.062X_5$$

$$SSA = 2.394 - 6.816X_1 + 0.002X_2 + 5.041X_3 - 0.006X_4 + 0.014X_5$$

The pareto charts of standardized effects on MC (Figure 1A) and SSA (Figure 1B) are shown. The limit

**Table 4** The Chemical Properties of Spray Dried PNS Powders in the Plackett-Burman Design

Runs	$X_1$	$X_2$	$X_3$	$X_4$	$X_5$	$R_1/\%$	$R_{g1}/\%$	$R_e/\%$	$R_{b1}/\%$	$R_d/\%$	Total Saponin/%
$S_1$	+1	-1	-1	-1	+1	8.98	29.37	2.64	34.56	8.50	84.05
$S_2$	+1	+1	+1	-1	-1	8.86	29.36	2.89	34.22	8.41	83.75
$S_3$	+1	+1	-1	-1	-1	8.35	28.31	3.58	32.23	7.92	80.39
$S_4$	-1	+1	-1	+1	+1	9.04	29.82	3.05	34.70	8.53	85.14
$S_5$	-1	+1	+1	+1	-1	8.82	29.75	3.75	33.91	8.34	84.56
$S_6$	-1	-1	-1	+1	-1	8.70	28.63	3.05	33.41	8.21	82.00
$S_7$	-1	-1	-1	-1	-1	9.08	30.59	3.80	34.81	8.55	86.83
$S_8$	-1	+1	+1	-1	+1	9.02	30.46	3.84	34.58	8.50	86.40
$S_9$	+1	-1	+1	+1	+1	9.08	30.73	3.61	35.13	8.67	87.21
$S_{10}$	+1	-1	+1	+1	-1	8.83	29.81	3.69	33.76	8.34	84.43
$S_{11}$	-1	-1	+1	-1	+1	9.05	30.32	3.34	35.01	8.61	86.33
$S_{12}$	+1	+1	-1	+1	+1	9.33	32.68	4.58	36.06	8.86	91.52
Max/Min	-	-	-	-	-	1.12	1.15	1.73	1.12	1.12	1.14

**Table 5** The Physical Properties of Spray Dried PNS Powders in the Plackett-Burman Design

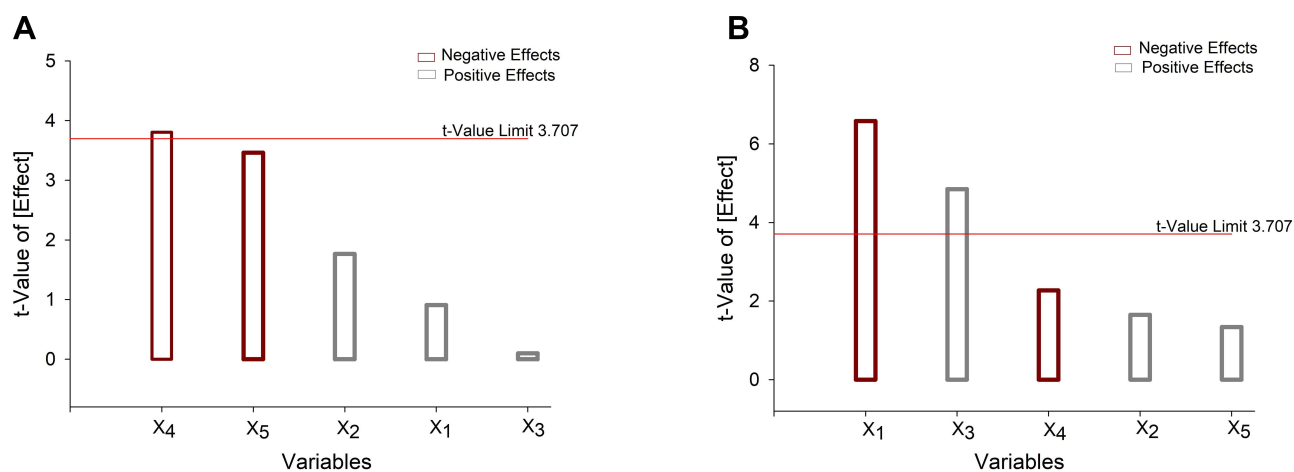
Runs	X <sub>1</sub>	X <sub>2</sub>	X <sub>3</sub>	X <sub>4</sub>	X <sub>5</sub>	Yield/%	MC/%	HI/%	SSA/m <sup>3</sup> /g	Span
S <sub>1</sub>	+1	-1	-1	-1	+1	70.8	3.94	9.05	0.64	1.82
S <sub>2</sub>	+1	+1	+1	-1	-1	56.2	5.79	7.41	1.35	1.49
S <sub>3</sub>	+1	+1	-1	-1	-1	74.6	5.22	7.85	0.63	1.24
S <sub>4</sub>	-1	+1	-1	+1	+1	79.1	2.58	10.49	1.27	1.03
S <sub>5</sub>	-1	+1	+1	+1	-1	62.1	3.96	7.45	2.79	1.16
S <sub>6</sub>	-1	-1	-1	+1	-1	68.7	3.43	9.19	1.23	1.16
S <sub>7</sub>	-1	-1	-1	-1	-1	69.6	3.62	7.63	1.67	1.11
S <sub>8</sub>	-1	+1	+1	-1	+1	67.0	3.12	8.20	3.45	1.25
S <sub>9</sub>	+1	-1	+1	+1	+1	75.4	2.01	9.63	0.87	0.94
S <sub>10</sub>	+1	-1	+1	+1	-1	68.9	2.79	9.24	0.87	1.11
S <sub>11</sub>	-1	-1	+1	-1	+1	72.1	3.39	7.76	3.06	1.09
S <sub>12</sub>	+1	+1	-1	+1	+1	65.4	2.36	7.99	0.92	1.17
Max/Min	-	-	-	-	-	1.4	2.88	1.42	5.50	1.94

of *t* value was estimated at the 99% confidence level. The *t* values of feed concentration (X<sub>1</sub>), atomization pressure (X<sub>3</sub>), and inlet air temperature (X<sub>4</sub>) were above the corresponding *t* value limits, indicating that the influences of the three parameters were statistically significant. Therefore, the feed concentration, atomization pressure, and inlet air temperature were identified as critical process parameters of the spray drying process.

### Effects of Critical Process Parameters on Properties of Spray Dried Powders

According to the Box-Behnken design in Preparation and Characterization of Spray Dried PNS Powders, 17 batches of experiments were carried out. The non-critical variable of feed flow rate X<sub>2</sub> was set as 500 mL/h, and the air flow rate X<sub>5</sub> was set as 60 m<sup>3</sup>/min. Table 6 shows the results of chemical quality attributes of spray dried PNS powders.

The content ranges were 8.43–8.88%, 28.43–29.84%, 3.78–4.25%, 34.04–41.94%, 7.97–8.39%, and 84.16–91.25% for notoginsenoside R<sub>1</sub>, ginsenoside Rg<sub>1</sub>, ginsenoside Re, ginsenoside Rb<sub>1</sub>, ginsenoside Rd, and total saponins, respectively. For each chemical quality attribute, the Max/Min value was close to 1, indicating that the difference of content between batches was not obvious. The analysis of variance for linear regression models in prediction of different chemical indices was performed, and the *p*-values of notoginsenoside R<sub>1</sub>, ginsenoside Rg<sub>1</sub>, ginsenoside Re, ginsenoside Rb<sub>1</sub>, ginsenoside Rd, and total saponins were 0.6346, 0.4921, 0.1896, 0.4737, 0.4869, and 0.2991, respectively. They were all greater than 0.1, revealing that the chemical properties were not significantly affected by changes in critical process parameters of spray drying. This was consistent with results in the screening experiments.

**Figure 1** The Pareto chart of standardized effects on the MC (A) and SSA (B).

**Table 6** The Chemical Properties of Spray Dried PNS Powders in the Box-Behnken Design

Runs	X <sub>1</sub>	X <sub>3</sub>	X <sub>4</sub>	R <sub>1</sub> /%	R <sub>g1</sub> /%	Re/%	Rb <sub>1</sub> /%	Rd/%	Total Saponin/%
S <sub>1</sub>	0	+1	-1	8.56	28.62	3.87	37.86	8.05	86.95
S <sub>2</sub>	+1	-1	0	8.43	28.43	3.96	37.46	7.97	86.25
S <sub>3</sub>	0	0	0	8.64	29.09	3.93	38.50	8.15	88.31
S <sub>4</sub>	0	0	0	8.83	29.70	4.03	39.33	8.35	90.24
S <sub>5</sub>	0	-1	+1	8.88	29.84	4.07	39.45	8.39	90.63
S <sub>6</sub>	+1	0	+1	8.78	29.45	4.11	38.89	8.26	89.49
S <sub>7</sub>	0	0	0	8.71	28.86	3.78	38.28	8.15	87.78
S <sub>8</sub>	-1	-1	0	8.73	29.06	4.25	38.31	8.14	88.49
S <sub>9</sub>	+1	0	-1	8.69	28.77	3.97	38.27	8.08	87.77
S <sub>10</sub>	-1	0	+1	8.67	28.73	3.96	38.06	8.05	87.46
S <sub>11</sub>	0	0	0	8.70	29.03	4.04	38.29	8.08	88.13
S <sub>12</sub>	0	-1	-1	8.71	28.97	3.94	38.44	8.13	88.18
S <sub>13</sub>	0	+1	+1	8.71	29.16	3.97	38.54	8.21	88.60
S <sub>14</sub>	-1	+1	0	8.56	28.67	3.98	41.94	8.10	91.25
S <sub>15</sub>	0	0	0	8.86	29.63	4.04	37.56	8.25	88.33
S <sub>16</sub>	-1	0	-1	8.76	29.27	3.91	34.04	8.19	84.16
S <sub>17</sub>	+1	+1	0	8.66	28.91	3.93	38.19	8.09	87.79
Max/Min				1.05	1.05	1.12	1.23	1.05	1.08

17 physical properties were measured according to Preparation and Characterization of Spray Dried PNS Powders for each batch of powder, as shown in Table 7. The values of  $Da$  and  $Dc$  were in the ranges of 0.07–0.19 g/mL and 0.1–0.29 g/mL, respectively, which meant the powder was porous. The range of  $Ds$  was between 1.16 g/mL and 1.31 g/mL, implying that when removing the external pores between particles, the densities of the powder in different batches varied within a small range. The indexes of  $IH$  and  $\alpha$  represented the flowability of the powder, if the angle of repose was less than 45°, it indicated that the powder had acceptable flowability. In this work, all spray dried powders had poor flowability ( $\alpha > 50^\circ$ ,  $IH > 1.4$ ). The indexes of  $Ie$ ,  $IC$  and  $Icd$  represented the compressibility of the powder. Good compressibility was beneficial to the formation of tablets. The measured ranges of  $Ie$ ,  $IC$  and  $Icd$  were 1.59–5.07, 29.54–43.74 and 133.0–213.4 N, respectively, which meant favorable hardness of prepared tablets would be obtained. The moisture contents of all powder samples were less than 3.5%, and the hygroscopicity was about 10%, indicating that the spray drying conditions could maintain product moisture at relatively low level, but the powder had the tendency to absorb moisture moderately. The glass transition temperatures are obtained from DSC thermograms as shown in Figure S1. The  $Tg$  values of spray dried PNS powders were quite high, ranging from 138.8°C to 142.7°C. The low moisture contents and glass transition temperatures

above the storage temperature (eg room temperature) were beneficial to the stability of powder product.<sup>38,39</sup>  $D_{10}$ ,  $D_{50}$ ,  $D_{90}$  and  $Span$  were parameters describing the particle sizes and distribution. The median particle sizes of all powders were about 5 $\mu$ m, and the  $Span$  values were between 1.30 and 1.54, indicating that the particle size of the powder was small and the particle size distribution was uniform. In addition, powders with small particle size would have large specific surface area. For instance, the spray dried PNS powders prepared in Run S<sub>2</sub> has the largest  $D_{50}$  value (6.99 $\mu$ m) but the smallest SSA (0.53 m<sup>2</sup>/g). In contrary, the spray dried PNS powders prepared in Run S<sub>14</sub> has the smallest  $D_{50}$  value (4.36 $\mu$ m) but the largest SSA (2.81 m<sup>2</sup>/g).

Furthermore, the linear and quadratic regression models were used to predict the powder properties. The linear model accounts only for the main effects. The applied quadratic model contains all terms that are the main effect terms, the two factor interaction terms and the second order terms. In prediction of a selected response, the best model is chosen in view of following considerations: (1) The model is statistically significant and the lack of fit is insignificant; (2) If both the linear and quadratic models meet the requirements, a model with larger adjusted determination coefficient is used. In prediction of  $Span$ ,  $IH$ ,  $IC$ ,  $Icd$ ,  $Ds$  and  $Tg$ , either the linear or the quadratic models were not significant (ie the p-values were larger than 0.05). This implied that the experimental factors did not impact



Table 7 The Physical Properties of Spray Dried PNS Powders in the Box-Behnken Design

Runs	Da (g/mL)	Yield (%)	Dc (g/mL)	Ds (g/mL)	D <sub>10</sub> (μm)	D <sub>50</sub> (μm)	D <sub>90</sub> (μm)	Span	IH	α (°)	Ie (%)	IC	Icd (N)	SSA (m <sup>2</sup> /g)	MC (%)	H (%)	Tg (°)
S <sub>1</sub>	0.19	65.53	0.26	1.22	2.67	5.61	10.18	1.34	1.42	53.02	1.59	29.54	194.8	1.76	3.31	8.85	142.7
S <sub>2</sub>	0.14	60.28	0.24	1.26	2.93	6.99	13.73	1.54	1.63	51.25	2.66	38.54	135.8	0.53	2.49	9.34	140.0
S <sub>3</sub>	0.13	74.10	0.21	1.28	2.74	5.93	11.08	1.41	1.62	55.07	2.91	38.40	186.9	0.83	2.16	9.92	141.2
S <sub>4</sub>	0.13	74.61	0.21	1.23	2.53	5.53	10.46	1.45	1.56	54.13	2.67	35.73	189.6	0.97	1.99	11.02	141.7
S <sub>5</sub>	0.09	72.27	0.15	1.31	2.85	6.16	11.43	1.39	1.62	56.27	4.18	38.40	181.0	0.74	1.73	11.50	138.8
S <sub>6</sub>	0.10	69.77	0.15	1.31	2.77	5.94	11.24	1.43	1.47	57.08	3.19	32.01	186.2	0.74	1.50	11.70	141.1
S <sub>7</sub>	0.12	73.31	0.19	1.26	2.72	5.72	10.28	1.32	1.59	59.14	3.10	37.07	188.3	0.84	1.82	11.01	140.5
S <sub>8</sub>	0.09	76.58	0.14	1.16	2.78	6.06	11.21	1.39	1.57	57.46	4.12	36.14	191.7	1.76	2.31	11.05	141.7
S <sub>9</sub>	0.19	67.05	0.29	1.28	3.09	6.72	11.97	1.34	1.54	55.14	1.88	35.21	145.6	1.14	2.92	10.12	141.4
S <sub>10</sub>	0.07	77.66	0.10	1.21	2.62	5.49	10.04	1.35	1.51	56.20	5.07	33.87	170.5	1.58	1.81	10.97	140.4
S <sub>11</sub>	0.11	74.34	0.18	1.24	2.68	5.47	10.01	1.34	1.58	55.02	3.19	36.55	157.8	1.02	2.12	10.73	140.4
S <sub>12</sub>	0.14	68.36	0.24	1.30	3.14	6.88	12.11	1.30	1.70	56.84	2.96	41.06	133.0	0.80	2.98	10.19	141.6
S <sub>13</sub>	0.09	73.85	0.13	1.29	2.61	5.36	9.84	1.35	1.46	56.72	3.52	31.34	153.4	0.96	1.55	11.26	140.1
S <sub>14</sub>	0.10	69.05	0.15	1.28	1.97	4.36	7.87	1.35	1.57	54.81	3.73	36.27	213.4	2.81	3.12	10.45	139.6
S <sub>15</sub>	0.12	73.26	0.19	1.29	2.45	5.19	9.75	1.41	1.59	55.86	3.18	37.20	173.0	1.03	1.84	10.45	140.2
S <sub>16</sub>	0.12	74.05	0.19	1.27	2.67	5.53	9.90	1.31	1.62	54.85	3.24	38.40	168.5	2.06	2.58	9.58	140.0
S <sub>17</sub>	0.13	69.00	0.23	1.25	2.33	5.33	10.11	1.46	1.78	52.94	3.40	43.74	165.3	0.70	1.99	10.43	139.4

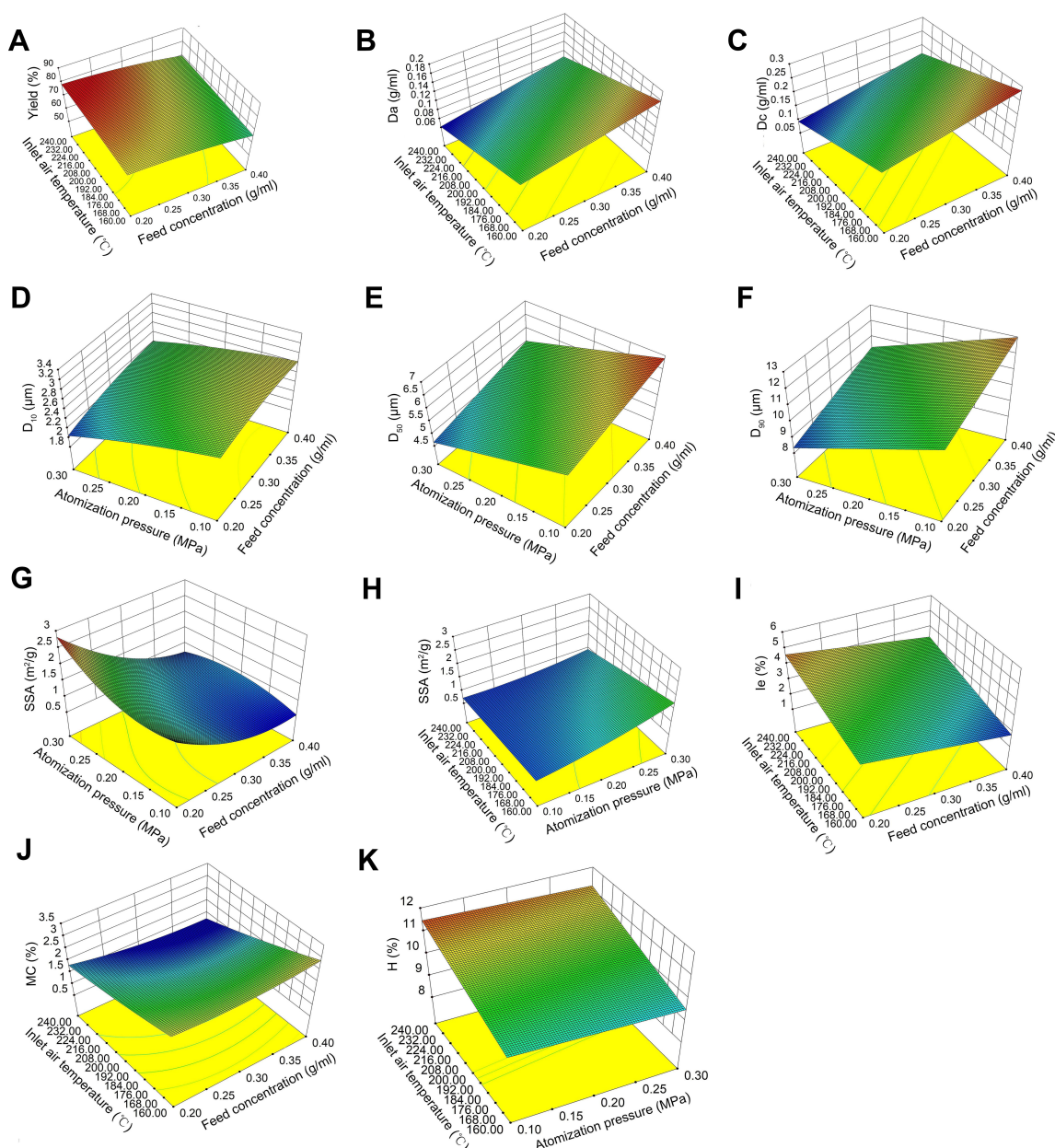
these response variables. Table 8 summarizes the modeling results for significant models ( $p$ -value $<0.05$ ). The quadratic models were built for two indexes of yield and MC, and the linear models were selected for  $H$ ,  $Da$ ,  $Dc$ ,  $Ie$ ,  $D_{90}$  and  $D_{50}$ . For  $D_{10}$ , both the linear and the quadratic models were fit for purpose, so the quadratic model with larger adjustment  $R^2$  of 0.7578 was selected as the optimal model. It should be noted that the cubic model was used to fit the experimental data of SSA, where it was found that both the linear and quadratic models were significant (ie  $p$ -values were 0.0004 and 0.0016, respectively) but the lack of fit test were also significant (ie  $p$ -values were 0.0073 and 0.0203, respectively). The lack of fit represented the probability that the actual value of the model did not fit the predicted value.<sup>40</sup> In order to reduce the significance of the lack-of-fit term, we added one higher-order term  $X_1X_3^2$  that had impacts on the model. The backward regression was applied to maximize the adjusted coefficient of determination, and to avoid overfitting. As a result, it turned out that the model  $p$ -value became  $<0.0001$  and the  $p$ -value of lack-of-fit term became 0.9626. This meant that the model was significant and the lack of fit term was not significant, which was reasonable for application. The coefficient of variation (CV) was calculated by the ratio of the standard deviation to the mean, and it indicated the degree of dispersion of the model data. The CV values of  $Da$  and  $Ie$  were larger than that of other indexes, showing that the data fluctuated greatly for the two properties. Adeq precision was called signal-to-noise ratio. In Table 8, the Adeq precision values are all greater than 4, indicating that the established models could truly reflect the results.<sup>41</sup>

Figure 2 depicts the 3D response surface plots, which are helpful for visually judging the extent of interactions between factors by the degree of curvature of the surface.

A large degree of curvature indicates obvious interactions. While, a steep surface indicates that the factor has an obvious influence on the response. Figure 2A shows the effects of the inlet air temperature and the feed concentration on the yield. Under the conditions of lower feed liquid concentration and higher inlet air temperature, it was expected that the material had more time and ability to dry to lower moisture content and the probability of sticking to the wall could be reduced.<sup>42</sup> The curvature of the surface in Figure 2A is small, indicating that the interaction between the two factors is not obvious. Figure 2B and C clearly show that when the feed concentration is reduced and the inlet air temperature is increased, both  $Da$  and  $Dc$  are decreased. The rapid decline of the curve confirmed that the two factors had large impacts on  $Da$  and  $Dc$ . This result is consistent with Figure 2I, where an opposite tendency occurs for the inter particle porosity. Figure 2D–F show that the particle size parameters have significant correlations with the feed concentration and the atomization pressure. The higher atomization pressure helped the atomizer to generate higher energy to break the large droplets into finer droplets, so the particle sizes of powders were likely to become smaller. The higher feed concentration increased the amount of the solids entering the atomizer per unit time, and it was not easy to break large droplets under the same energy, so the particle size increased. In Figure 2G and H, it can be observed that the specific surface area is positively related to the atomization pressure, and is negatively related with the feed concentration and the inlet air temperature. All the three CPPs had impacts on SSA, and the interaction between the feed concentration and the atomization pressure as well as the interaction between the atomization pressure and the inlet air temperature were obvious. Besides, inlet air temperature is negatively

**Table 8** The ANOVA Results and Model Quality Metrics for Optimized Regression Models

Index	Model Type	Model p-value	Lack of Fit p-value	CV/%	$R^2$	$R^2_{adj}$	Adeq Precision
Yield	Quadratic	$<0.0001$	0.0818	1.39	0.9781	0.9500	23.48
$Da$	Linear	$<0.0001$	0.1966	10.53	0.8741	0.8450	19.11
$Dc$	Linear	$<0.0001$	0.5387	7.71	0.9313	0.9154	26.94
$D_{10}$	Quadratic	0.0107	0.4003	5.02	0.8940	0.7578	11.40
$D_{50}$	Linear	$<0.0001$	0.4038	5.36	0.8192	0.7775	14.92
$D_{90}$	Linear	$<0.0001$	0.4407	5.16	0.8489	0.8141	17.34
$Ie$	Linear	0.0001	0.0719	13.18	0.7834	0.7334	13.75
SSA	Cubic	$<0.0001$	0.9626	6.06	0.9928	0.9857	43.26
MC	Quadratic	0.0016	0.1677	9.26	0.9402	0.8634	12.26
$H$	Linear	0.0063	0.3505	5.18	0.6004	0.5082	7.38



**Figure 2** The 3D response surface plots depicting the effects of critical process parameters on different physical properties ((A) process yield; (B) bulk density; (C) tapped density; (D)  $D_{10}$ ; (E)  $D_{50}$ ; (F)  $D_{90}$ ; (G and H) specific surface area; (I) inter-particle porosity; (J) moisture content; (K) hygroscopicity).

correlated with MC, and positively correlated with H, as shown in Figure 2J and K. A thorough understanding of relationships between critical process parameters and physical quality attributes of the spray dried powder was conducive to flexible adjustment of the process conditions.

## Dissolution Behavior of PNS Tablets

According to In vitro Dissolution Test, the dissolution test was performed. The cumulative release of APIs in 17 batches of PNS hydrophilic matrix tablets were calculated

using Equations (10) and (11). Within the same batch, the  $f_2$  factors of either two dissolution curves of five APIs were larger than 50, indicating that these ingredients released synchronously within the 0–12 h. Hence, the ginsenoside  $Rg_1$  was used as an example to describe the change of PNS release over time. The cumulative release profiles of ginsenoside  $Rg_1$  for 17 batches of PNS hydrophilic matrix tablets are shown in Figure 3. The Higuchi, the Korsmeyer-Peppas and the zero order models were used to fit the dissolution curve. The determination coefficients of the Korsmeyer-Peppas models were all greater

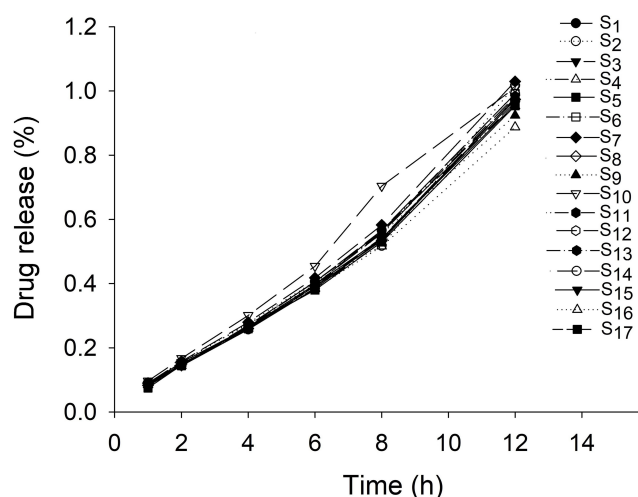


Figure 3 The cumulative drug release profiles of ginsenoside Rg<sub>1</sub>.

than 0.98 except for S<sub>2</sub> ( $R^2=0.9784$ ). The release exponents of the Korsmeyer-Peppas model were from 1.05 to 1.23, indicating the release mechanism of super case II transport.<sup>43</sup> S<sub>10</sub> had higher drug release rate than other conditions. It was inferred from the Box-Behnken design that the drug release amount was high when inlet air temperature was at the high level, and feed concentration and atomization pressure were at low and medium levels respectively.

### Effects of Critical Process Parameters on Intra-Batch Variability of Drug Release

A thorough investigation of effects of critical process parameters on dissolution of different APIs at 12 h was performed, but none significant correlations were observed for any components. Furtherly, a phenomenon of intra-batch variability was observed. For a particular component, the intra-batch variability referred to the relative standard deviation (RSD) of the dissolution between six tablets in a same batch. The ANOVA of intra-batch variability prediction models at different time points were carried out. The results showed that except for 12h (p-value 0.0962), the model p-values at 1, 2, 4, 6, 8h were 0.1505, 0.3056, 0.3467, 0.3137 and 0.1790 respectively, which were all greater than 0.1, indicating that the process parameters have a significant effect on the intra-batch dissolution variability in 12h. Therefore, the time point of 12 h was used. For instance, as shown in Table 9, the intra-batch dissolution variability of notoginseng saponins Rg<sub>1</sub> varies from 0.5% to 7.3%. The overall within batch robustness of PNS tablet was evaluated by the average

Table 9 The Intra-Batch Dissolution Variability of Five APIs in the Box-Behnken Design

Runs	R <sub>1</sub>	Rg <sub>1</sub>	Re	Rb <sub>1</sub>	Rd	Average
S <sub>1</sub>	0.056	0.055	0.055	0.062	0.065	0.058
S <sub>2</sub>	0.044	0.044	0.047	0.048	0.051	0.047
S <sub>3</sub>	0.044	0.040	0.040	0.046	0.054	0.045
S <sub>4</sub>	0.024	0.020	0.026	0.024	0.023	0.024
S <sub>5</sub>	0.044	0.046	0.056	0.050	0.055	0.050
S <sub>6</sub>	0.020	0.021	0.049	0.019	0.022	0.026
S <sub>7</sub>	0.016	0.014	0.067	0.017	0.018	0.026
S <sub>8</sub>	0.061	0.060	0.077	0.066	0.079	0.069
S <sub>9</sub>	0.054	0.059	0.076	0.065	0.083	0.068
S <sub>10</sub>	0.013	0.005	0.014	0.007	0.016	0.011
S <sub>11</sub>	0.070	0.073	0.105	0.074	0.094	0.083
S <sub>12</sub>	0.067	0.069	0.082	0.072	0.074	0.073
S <sub>13</sub>	0.016	0.017	0.060	0.021	0.023	0.027
S <sub>14</sub>	0.026	0.025	0.090	0.026	0.056	0.044
S <sub>15</sub>	0.011	0.014	0.032	0.012	0.013	0.017
S <sub>16</sub>	0.062	0.066	0.159	0.066	0.072	0.085
S <sub>17</sub>	0.054	0.071	0.170	0.061	0.065	0.084

intra-batch dissolution variability of five APIs, which was ranged from 1.1% to 8.5%.

By using spray drying conditions as the independent variables, the intra-batch dissolution variability of notoginseng saponins Rg<sub>1</sub> and the intra-batch robustness of PNS tablet were modeled and predicted. The MLR models were good enough to fit such correlations. As shown in Table 10, the p-values of the two models are all less than 0.1, and the p-values of lack of fit are all greater than 0.1, indicating that the models are acceptable at the significance level of 0.1. The p-value of the inlet air temperature (X<sub>4</sub>) was smaller than 0.05, revealing that the inlet air temperature has significant effects on the intra-batch variability of dissolution. After a further look at the regression coefficients, it was found that the high inlet air temperature could decrease the intra-batch dissolution variability.

Figure 4 represents the spray drying process design space, where the yellow area means that both the intra-batch dissolution variability for notoginseng saponins Rg<sub>1</sub> and the average RSD values for five APIs were less than

Table 10 The ANOVA Results for the Linear Regression Model

RSD	Model	Model p-value	Lack of Fit p-value	p-value of Variable		
				X <sub>1</sub>	X <sub>3</sub>	X <sub>4</sub>
Rg <sub>1</sub>	Linear	0.0560	0.8668	0.4982	0.3609	0.0124
PNS	Linear	0.0962	0.8258	0.8042	0.6970	0.0164

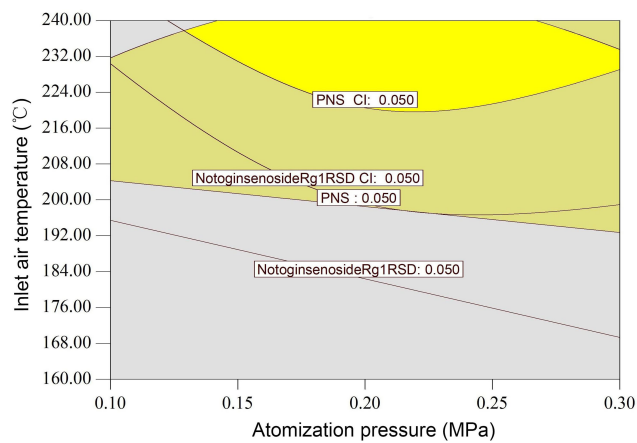


**Figure 4** The design space for consistent drug release of PNS matrix tablet.

5% after adding the 95% confidence interval. When the inlet air temperature was above 224°C, the intra-batch tablet release was considered to be consistent.

## Multivariate Analysis of Existing Data on Factors Affecting Intra-Batch Dissolution Variability

The three critical process parameters and their expanded terms (ie the cross and squares terms), together with 17 physical properties of the spray dried powder were used as independent variables. The average intra-batch dissolution variability of five APIs was used as the dependent variable. The partial least squares (PLS) regression model was used to correlate the independent and dependent variables. The first two latent variables explained 70% of the dependent variable information. Then, the variable importance in projection (VIP) values are evaluated, as shown in Figure 5. The variables with VIP value greater than 1 were the inlet air temperature ( $X_4$ ), MC, Dc, H, Da. IH, IC and the interaction terms of feed concentration and atomization pressure. However, the error bars of the latter three parameters were relatively large and crossed with the zero line, which meant that their contributions were uncertain. Therefore, the inlet air temperature had the greatest influence on the dissolution variability, followed by the moisture content and density related properties of the spray-dried powder.

Furthermore, the biplot is depicted in Figure 6, allowing us to interpret the relationships among different variables. It could be seen that the inlet air temperature ( $X_4$ ) was situated in the opposite position of the dependent variable, demonstrating that increasing inlet air

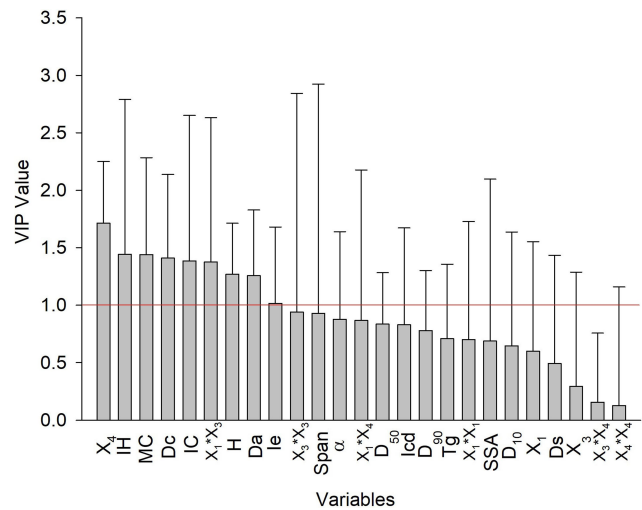


**Figure 5** Variable importance in projection for independent variables of the PLS model.

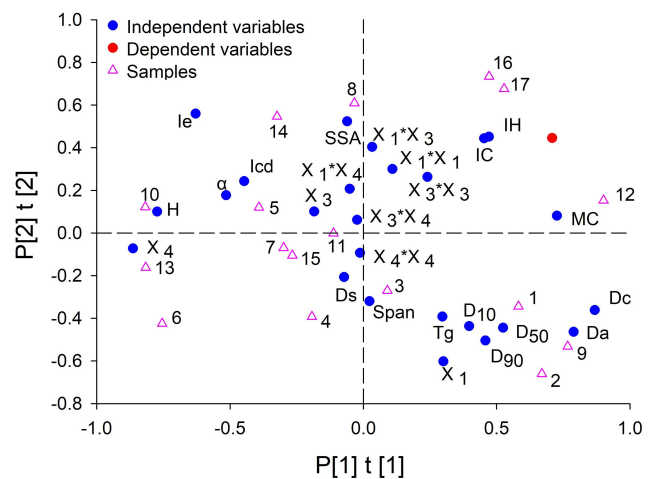


**Figure 6** The biplot of the PLS model.

temperature could decrease the intra-batch dissolution variability. The hygroscopicity was close to the inlet air temperature, while the moisture content was situated on the other side. This was consistent with the influences of the inlet air temperature on H and MC in Effects of Critical Process Parameters on Properties of Spray Dried Powders. The results also suggested that moisture content could account for the major reason for the intra-batch dissolution variability, from the aspect of powder physical properties. Water affected tablet dissolution by its interaction with APIs or excipients, as well as the tablet's porosity and mechanical strength.<sup>44,45</sup> A recent study by Okada et al showed that the sprayed water droplet had different evaporation rate, and the low drying air temperature would result in the spread of

unevaporated droplets throughout the drying tower.<sup>46</sup> The presence of water will produce dry and wet phases in the powder. Due to the phase change, the composition will be unevenly distributed, which will affect the uniformity of dissolution.<sup>47</sup>

## Conclusion

This study illustrated the effect of spray drying conditions on the intra-batch dissolution variability of the PNS hydrophilic matrix tablet containing high drug load of spray-dried PNS powder. First, three critical process parameters that were feed concentration, atomization pressure and inlet air temperature that affected the physical properties of spray dried powder were identified through the screening experimental design. Secondly, with the help of response surface methodology, it was found that the critical process parameters had little impact on chemical properties of spray dried PNS powder, but had greater impacts on powder physical properties such as particle size, specific surface area, etc. Furtherly, the dissolution behavior of PNS hydrophilic matrix tablets was clarified and the relationships between intra-batch dissolution variability and critical process parameters were investigated. The multivariate analysis results revealed that high inlet air temperature of spray drying process could produce PNS powders with low moisture and high hygroscopicity, which were beneficial to reduce the intra-batch dissolution variability. Our research provided a reference for improving the spray drying conditions in order to ensure the dissolution consistency of the PNS hydrophilic matrix tablet. In future, whether the modeled relationship will be reproduced in pilot or commercial scales of spray drying process, and whether such intra-batch dissolution variability will be propagated into the in vivo performance of PNS sustained release tablets, are worthy of further investigations.

## Acknowledgment

The authors are thankful to National Natural Science Foundation of China (No. 82074033) and Young Elite Scientists Sponsorship Program by CACM (No. 2019-QNRC2-C11).

## Author Contributions

All authors made a significant contribution to the work reported, whether that is in the conception, study design, execution, acquisition of data, analysis and interpretation, or in all these areas; took part in drafting, revising or

critically reviewing the article; gave final approval of the version to be published; have agreed on the journal to which the article has been submitted; and agree to be accountable for all aspects of the work.

## Disclosure

The authors report no conflicts of interest. The authors alone are responsible for the content and writing of this article.

## References

- World Health Organization [homepage on the Internet]. Cardiovascular diseases (CVDs); 2017. Available from: [https://www.who.int/en/news-room/factsheets/detail/cardiovascular-diseases-\(cvds\)](https://www.who.int/en/news-room/factsheets/detail/cardiovascular-diseases-(cvds)). Accessed February 5, 2021.
- Duan L, Xiong X, Hu J, Liu Y, Wang J. Efficacy and safety of oral Panax notoginseng saponins for unstable angina patients: a meta-analysis and systematic review. *Phytomedicine*. 2018;47:23–33. doi:10.1016/j.phymed.2018.04.044
- Mangalpally KK, Kleiman NS. The safety of clopidogrel. *Expert Opin Drug Saf*. 2011;10(1):85–95. doi:10.1517/14740338.2011.532485
- Pergolizzi JV, Coluzzi F, Colucci RD, et al. Statins and muscle pain. *Expert Rev Clin Pharmacol*. 2020;13(3):299–310. doi:10.1080/17512433.2020.1734451
- Lau AJ, Toh DF, Chua TK, Pang YK, Woo SO, Koh HL. Antiplatelet and anticoagulant effects of Panax notoginseng: comparison of raw and steamed Panax notoginseng with Panax ginseng and Panax quinquefolium. *J Ethnopharmacol*. 2009;125(3):380–386. doi:10.1016/j.jep.2009.07.038
- Yang X, Xiong X, Wang H, Wang J. Protective effects of Panax notoginseng saponins on cardiovascular diseases: a comprehensive overview of experimental studies. *Evid Based Complement Alternat Med*. 2014;2014:204840. doi:10.1155/2014/204840
- Pan C, Huo Y, An X, et al. Panax notoginseng and its components decreased hypertension via stimulation of endothelial-dependent vessel dilatation. *Vascul Pharmacol*. 2012;56(3–4):150–158. doi:10.1016/j.vph.2011.12.006
- Xia KP, Ca HM, Shao CZ. Protective effect of notoginsenoside R1 in a rat model of myocardial ischemia reperfusion injury by regulation of Vitamin D3 upregulated protein 1/NF-κB pathway. *Die Pharmazie*. 2015;70(11):740–744. doi:10.1691/ph.2015.5694
- Wang W, Yang L, Song L, et al. Combination of Panax notoginseng saponins and aspirin potentiates platelet inhibition with alleviated gastric injury via modulating arachidonic acid metabolism. *Biomed Pharmacother*. 2021;134:111165. doi:10.1016/j.biopha.2020.111165
- Sun F, Xu B, Dai S, Zhang Y, Lin Z, Qiao Y. A novel framework to aid the development of design space across multi-unit operation pharmaceutical processes—a case study of Panax notoginseng saponins immediate release tablet. *Pharmaceutics*. 2019;11(9):474. doi:10.3390/pharmaceutics11090474
- Li H, Li B, Zheng Y. Exploring the mechanism of action compound-xueshuantong capsule in diabetic retinopathy treatment based on network pharmacology. *Evid Based Complement Alternat Med*. 2020;2020:8467046. doi:10.1155/2020/8467046
- Lyu J, Xie Y, Sun M, Zhang L. Efficacy and safety of xueshuantong injection on acute cerebral infarction: clinical evidence and grade assessment. *Front Pharmacol*. 2020;11:822. doi:10.3389/fphar.2020.00822
- Polepally AR, Rimmel RP, Brundage RC, et al. Steady-state pharmacokinetics and bioavailability of immediate-release and extended-release formulations of lamotrigine in elderly epilepsy patients: use of stable isotope methodology. *J Clin Pharmacol*. 2015;55(10):1101–1108. doi:10.1002/jcph.522

14. Jin D, Wang B, Hu R, et al. A novel colon-specific osmotic pump capsule of *Panax notoginseng* saponins (PNS): formulation, optimization, and in vitro-in vivo evaluation. *AAPS PharmSciTech*. 2018;19(5):2322–2329. doi:10.1208/s12249-018-1068-2
15. Moussa E, Siepmann F, Flament MP, et al. Controlled release tablets based on HPMC: lactose blends. *J Drug Deliv Sci Technol*. 2019;52:607–617. doi:10.1016/j.jddst.2019.05.028
16. Gallo L, Pina J, Bucala V, Allemandi D, Ramirez-Rigo MV. Development of a modified-release hydrophilic matrix system of a plant extract based on co-spray-dried powders. *Powder Technol*. 2013;241:252–262. doi:10.1016/j.powtec.2013.03.011
17. Körner A, Piculell L, Iselau F, Wittgren B, Larsson A. Influence of different polymer types on the overall release mechanism in hydrophilic matrix tablets. *Molecules*. 2009;14(8):2699–2716. doi:10.3390/molecules14082699
18. Zahoor FD, Mader KT, Timmins P, Brown J, Sammon C. Investigation of within-tablet dynamics for extended release of a poorly soluble basic drug from hydrophilic matrix tablets using ATR-FTIR imaging. *Mol Pharm*. 2020;17(4):1090–1099. doi:10.1021/acs.molpharmaceut.9b01063
19. Yahoum MM, Lefnaoui S, Moulai-Mostefa N. Design and evaluation of sustained release hydrophilic matrix tablets of Piroxicam based on carboxymethyl xanthan derivatives. *Soft Mater*. 2020;1–14. doi:10.1080/1539445X.2020.1789994
20. Li Y, Zhang Y, Zhu CY. Pharmacokinetics and correlation between in vitro release and in vivo absorption of bio-adhesive pellets of *panax notoginseng* saponins. *Chin J Nat Med*. 2017;15(2):142–151. doi:10.1016/S1875-5364(17)30029-8
21. Peng Z. *Study on preparation technology and drug release in vitro and in vivo of total saponins sustained release tablets of Panax notoginseng* [Dissertation]. Hubei University of Traditional Chinese Medicine; 2012.
22. Stauffer F, Vanhoorne V, Pilcer G, et al. Raw material variability of an active pharmaceutical ingredient and its relevance for processability in secondary continuous pharmaceutical manufacturing. *Eur J Pharm Biopharm*. 2018;127:92–103. doi:10.1016/j.ejpb.2018.02.017
23. Thoorens G, Krier F, Rozet E, Carlin B, Evrard B. Understanding the impact of microcrystalline cellulose physicochemical properties on tabletability. *Int J Pharm*. 2015;490(1–2):47–54. doi:10.1016/j.ijpharm.2015.05.026
24. Zhang Y, Xu B, Wang X, et al. Setting up multivariate specifications on critical raw material attributes to ensure consistent drug dissolution from high drug-load sustained-release matrix tablet. *Drug Dev Ind Pharm*. 2018;44(11):1733–1743. doi:10.1080/03639045.2018.1492608
25. Zhang Y, Xu B, Wang X, Dai S, Shi X, Qiao Y. Optimal selection of incoming materials from the inventory for achieving the target drug release profile of high drug load sustained-release matrix tablet. *AAPS PharmSciTech*. 2019;20(2):76. doi:10.1208/s12249-018-1268-9
26. Salama AH. Spray drying as an advantageous strategy for enhancing pharmaceuticals bioavailability. *Drug Deliv Transl Res*. 2019;10(1):1–12. doi:10.1007/s13346-019-00648-9
27. Krishnaiah D, Bono A, Sarbatly R, Nithyanandam R, Anisuzzaman SM. Optimisation of spray drying operating conditions of *Morinda citrifolia* L. fruit extract using response surface methodology. *J King Saud Univ Sci*. 2015;27(1):26–36. doi:10.1016/j.jksues.2012.10.004
28. Santhalakshmy S, Bosco SJD, Francis S, Sabeena M. Effect of inlet temperature on physicochemical properties of spray-dried jamun fruit juice powder. *Powder Technol*. 2015;274:37–43. doi:10.1016/j.powtec.2015.01.016
29. Wang HM, Fu TM, Guo LW. The influence of spray drying process conditions on physical, chemical properties and lung inhaling performance of *Panax notoginseng* saponins - tanshinone II A composite particles. *Acta Pharm Sin B*. 2013;48(6):925–932.
30. A-sun K, Thumthanaruk B, Lekhavat S, Jumnonpon R. Effect of spray drying conditions on physical characteristics of coconut sugar powder. *Int Food Res J*. 2016;23(3):1315–1319.
31. Tontul I, Topuz A. Spray-drying of fruit and vegetable juices: effect of drying conditions on the product yield and physical properties. *Trends Food Sci Technol*. 2017;63:91–102. doi:10.1016/j.tifs.2017.03.009
32. Rattes ALR, Oliveira WP. Spray drying conditions and encapsulating composition effects on formation and properties of sodium diclofenac microparticles. *Powder Technol*. 2007;171(1):7–14. doi:10.1016/j.powtec.2006.09.007
33. Gagneten M, Corfield R, Mattson MG, et al. Spray-dried powders from berries extracts obtained upon several processing steps to improve the bioactive components content. *Powder Technol*. 2019;342:1008–1015. doi:10.1016/j.powtec.2018.09.048
34. Zambon A, Michelino F, Bourdoux S, et al. Microbial inactivation efficiency of supercritical CO<sub>2</sub> drying process. *Dry Technol*. 2018;36(16):2016–2021. doi:10.1080/07373937.2018.1433683
35. Pandey P, Dua K, Dureja H. Erlotinib loaded chitosan nanoparticles: formulation, physicochemical characterization and cytotoxic potential. *Int J Biol Macromol*. 2019;139:1304–1316. doi:10.1016/j.ijbiomac.2019.08.084
36. Administration USFD. Pharmacopeia of USA. Chapter 711: dissolution. 2017.
37. Zouari A, Mtibaa I, Triki M, et al. Effect of spray-drying parameters on the solubility and the bulk density of camel milk powder: a response surface methodology approach. *Int J Dairy Technol*. 2020;73(3):616–624. doi:10.1111/1471-0307.12690
38. Hang L, Zhou R, Mujumdar AS. Variation of glass transition temperature and control of product quality during spray drying. *Chem Ind Forest Prod*. 2007;27(1):43–46. doi:10.3321/j.issn:0253-2417.2007.01.010
39. Gallo L, Llabot JM, Allemandi D, Bucala V, Piña J. Influence of spray-drying operating conditions on *Rhamnus purshiana* (Cáscara sagrada) extract powder physical properties. *Powder Technol*. 2011;208(1):205–214. doi:10.1016/j.powtec.2010.12.021
40. Conde-Amboage M, Sanchez-Sellero C, Gonzalez-Manteiga W. A lack-of-fit test for quantile regression models with high-dimensional covariates. *Comput Stat Data Anal*. 2015;88:128–138. doi:10.1016/j.csda.2015.02.016
41. Chamoli S. ANN and RSM approach for modeling and optimization of designing parameters for a V down perforated baffle roughened rectangular channel. *Alex Eng J*. 2015;54(3):429–446. doi:10.1016/j.aej.2015.03.018
42. Roy S, Siddique S, Majumder S, et al. A systemic approach on understanding the role of moisture in pharmaceutical product degradation and its prevention: challenges and perspectives. *Biomed Res*. 2018;29(17):3336–3343. doi:10.4066/biomedicalresearch.29-18-978
43. Hansen CM. The significance of the surface condition in solutions to the diffusion equation: explaining “anomalous” sigmoidal, Case II, and Super Case II absorption behavior. *Eur Polym J*. 2010;46(4):651–662. doi:10.1016/j.eurpolymj.2009.12.008
44. Li S, Wei B, Fleres S, Comfort A, Royce A. Correlation and prediction of moisture-mediated dissolution stability for benazepril hydrochloride tablets. *Pharm Res*. 2004;21(4):617–624. doi:10.1023/b:pham.0000022408.91151.64
45. Gabbott IP, Al Husban F, Reynolds GK. The combined effect of wet granulation process parameters and dried granule moisture content on tablet quality attributes. *Eur J Pharm Biopharm*. 2016;106:70–78. doi:10.1016/j.ejpb.2016.03.022
46. Okada S, Ohsaki S, Nakamura H, Watano S. Estimation of evaporation rate of water droplet group in spray drying process. *Chem Eng Sci*. 2020;227:115938. doi:10.1016/j.ces.2020.115938
47. Gal S. Recent developments in techniques for obtaining complete sorption isotherms. In: Rockland LB, Stewart GF, editors. *Water Activity Influences on Food Quality*. California:Academic Press; 1981:89–110. doi:10.1016/B978-0-12-591350-8.50009-7

## Drug Design, Development and Therapy

Dovepress

### Publish your work in this journal

Drug Design, Development and Therapy is an international, peer-reviewed open-access journal that spans the spectrum of drug design and development through to clinical applications. Clinical outcomes, patient safety, and programs for the development and effective, safe, and sustained use of medicines are a feature of the journal, which has also

been accepted for indexing on PubMed Central. The manuscript management system is completely online and includes a very quick and fair peer-review system, which is all easy to use. Visit <http://www.dovepress.com/testimonials.php> to read real quotes from published authors.

Submit your manuscript here: <https://www.dovepress.com/drug-design-development-and-therapy-journal>